

Photoluminescence of erbium-doped silicon: Excitation power and temperature dependence

D. T. X. Thao,^{a)} C. A. J. Ammerlaan,^{b)} and T. Gregorkiewicz

Van der Waals-Zeeman Institute, University of Amsterdam, Valckenierstraat 65, NL-1018 XE Amsterdam, The Netherlands

(Received 25 May 1999; accepted for publication 18 April 2000)

Photoluminescence measurements have been made on float-zone and Czochralski-grown silicon samples which were doped with erbium by ion implantation. The characteristic luminescence spectra in the wavelength range between 1.5 and 1.6 μm were observed. Differences in the multiple line structure of the spectra indicated that the active luminescent centers have different symmetries and atomic structure. The dependence of the photoluminescence intensity on the laser excitation power and on the temperature was measured. Results are discussed on the basis of a physical model which includes the formation of free excitons, the binding of excitons to erbium ions, the excitation of 4*f* inner-shell electrons of the erbium ions, and their subsequent decay by light emission. To obtain a quantitative agreement between model analysis and experimental data the consideration of Auger processes by which erbium-bound excitons and erbium ions in excited state can decay by dissipating energy to conduction band electrons appears to be required. From the temperature dependence two activation energies are derived which are associated with the exciton binding energies and with an energy transfer process from excited erbium ions back to erbium-bound excitons, respectively. A good quantitative agreement can be obtained for suitable values of the model parameters. The luminescent properties of the samples of the different types of crystalline silicon are remarkably similar. © 2000 American Institute of Physics. [S0021-8979(00)00415-1]

I. INTRODUCTION

In recent years much research activity has been devoted to rare-earth impurities in silicon and semiconductor compounds with the objective of investigating basic physical properties and developing related electro-optical applications.¹ Erbium-doped silicon is intensively investigated since the luminescence of erbium occurs in the wavelength region of minimum loss and dispersion of glass fibers.

The characteristic luminescence of erbium is due to electronic transitions within the 4*f* shell between states of which energy differences are primarily determined by spin-orbit coupling. For an isolated erbium ion the electric dipole transitions between such states are not allowed. In a silicon crystal the transitions become possible if, due to the presence of a ligand field, the local symmetry is lowered and states of opposite parity become mixed. It has been found that Er ions can be incorporated in silicon on sites of different symmetries²⁻⁴ and have strong propensity to form complexes with other impurities.⁵ This gives rise to structurally different erbium-related centers which are characterized by individual luminescence spectra.⁶ For the formation of complexes, the presence of oxygen appears to be especially important.⁷⁻⁹ It has been reported that the photoluminescence (PL) intensity of Er- and Er,O-doped Czochralski silicon (Cz-Si) is always higher than that observed in float-zone silicon (Fz-Si).^{10,11} The particular role of oxygen as a codopant in the enhance-

ment of erbium-related PL is, however, not established in sufficient detail. In an extended x-ray absorption fine structure study Adler *et al.*¹² found that the first-neighbor shell of the erbium ion in Cz-Si comprises four to six oxygen atoms which are responsible for the optical activity of the complex. In Fz-Si an erbium ion is surrounded by twelve silicon atoms yielding an optically inactive complex. Based on these results they concluded that the higher intensity in Cz-Si is due to the formation of erbium-oxygen complexes. Przybylinska *et al.*^{13,14} identified more than 100 distinct lines in PL spectra of erbium-implanted silicon and ascribed them to different types of erbium centers: Isolated erbium ions at cubic and noncubic symmetry sites, erbium-oxygen complexes, and centers related to clusters of erbium with residual radiation defects. All these results underline the relevance of the specific role of oxygen in the formation of optically active erbium centers and the enhancement of the luminescence yield.

Valuable information on the excitation and de-excitation mechanisms can be deduced from the dependence of the photoluminescence intensity on the excitation power and the temperature. Priolo *et al.*¹⁵ found that impurity codoping, such as with O, F, or C, reduced the temperature quenching of the PL yield. In this particular study the temperature effect was ascribed to thermalization of electrons bound at the erbium or erbium-related donor center with the conduction band. In the PL temperature dependence measured for an oxygen-rich material grown by molecular beam epitaxy and containing erbium and oxygen to concentrations of $2 \times 10^{19} \text{ cm}^{-3}$ and 10^{19} cm^{-3} , respectively, Efeoglu *et al.*¹⁶ identified three temperature quenching mechanisms and related them to different microscopic processes. A comprehen-

^{a)}Also at: International Training Institute for Materials Science, ITIMS Building, Dai hoc Bach Khoa Hanoi, 1 Dai Co Viet Road, Hanoi, Vietnam

^{b)}Electronic mail: ammerlaan@wins.uva.nl

sive and more quantitative theoretical treatment of the energy transfer, also accounting for temperature effects, was developed by Bresler *et al.*¹⁷ Recently, Palm *et al.*¹⁸ proposed a set of rate equations to describe the photoluminescence of erbium in silicon and pointed out the importance of nonradiative energy transfer processes involving conduction band electrons.

In the present article we present photoluminescence measurements on both float-zone, oxygen lean, and Czochralski-grown, oxygen-rich, silicon samples doped with erbium. Some contrasting results obtained on an amorphous sample are reported as well. By the multiple component structure in the spectra the existence of erbium-related centers of different symmetry, cubic and noncubic, is confirmed. The temperature and laser power dependencies were measured and are described by an excitation mechanism involving free and bound exciton intermediate states. Results are analyzed on the basis of a model with the aim of verifying the quantitative agreement.

II. EXPERIMENT

In the experiments the following four kinds of material were used:

(1) Float-zone, *n*-type phosphorus-doped, $\langle 100 \rangle$ oriented silicon wafers, labeled Fz-Si:Er. The room-temperature resistivity of this material was 0.7–0.9 Ω cm. The samples were implanted with erbium ions at an energy of 1.1 MeV to total doses in the range of 1×10^{12} – 5×10^{15} cm⁻². Implantations were performed at 500 °C. No additional heat treatment has been applied.¹⁹

(2) A *p*-type Czochralski-grown silicon sample with oxygen concentration of 2×10^{18} cm⁻³. The sample was implanted with erbium ions at an energy of 320 keV, with the dose 5×10^{12} cm⁻² corresponding to an erbium peak concentration of 5×10^{17} cm⁻³. Samples are designated as Cz-Si:Er.

(3) Other *p*-type Cz-Si material with the room-temperature resistivity of 1–10 Ω cm. Wafers were implanted with erbium ions, with energy of 1.2 MeV, to a dose of 10^{13} cm⁻² and coimplanted with oxygen ions of energy 0.17 MeV to a dose of 10^{14} cm⁻². Such samples are labeled Cz-Si:Er,O. To optimize the luminescence output the samples were subsequently annealed for 0.5 h at the temperature of 900 °C in a chlorine-containing atmosphere.^{20,21}

(4) Amorphous silicon samples produced by magnetron-assisted silane decomposition on a crystalline silicon substrate. Erbium concentrations in these films reach 10^{20} cm⁻³. Samples are designated by a-Si:Er.²²

The luminescence was excited by the 514 nm line of an Ar⁺-ion laser (Spectra-Physics Stabilite 2016-05s). The laser power could be varied from 0.1 to 1000 mW. This corresponded to an excitation power in the spot of about 1 mm diameter measured in front of the sample in the range from 1 μ W to 10 mW. The emitted light was dispersed by a high-resolution 1.5 m *F*/12 grating monochromator (Jobin-Yvon THR 1500) and detected by a liquid-nitrogen cooled North-Coast EO-817 germanium detector. Variation of the PL yield as a function of excitation power was measured with the sample immersed in liquid helium. For the measurements of

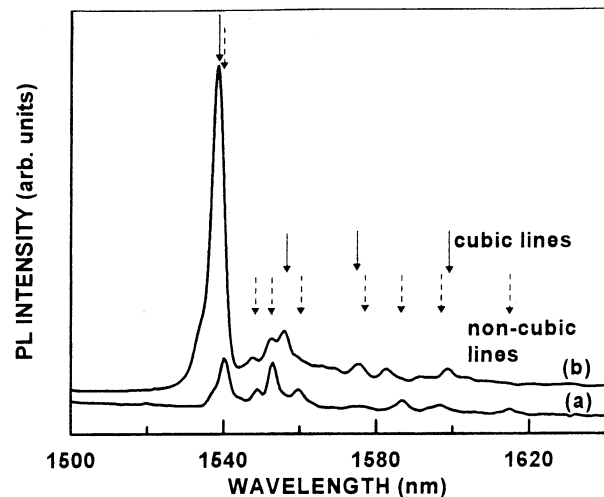


FIG. 1. Photoluminescence spectra measured at 4.2 K for (a) sample of Fz-Si:Er and (b) sample of Cz-Si:Er,O. Solid arrows indicate spectral components due to emission of the cubic center, mainly present in the Czochralski silicon, broken arrows label the eight components belonging to a center of lower symmetry prevailing in the float-zone silicon.

the temperature dependence of the PL intensity an Oxford Instruments cryostat with a variable temperature insert was used. The temperature of the samples was measured by a RhFe metallic resistor in a four-point-probe configuration to an accuracy of 0.1 K. Temperature control was achieved by proportional integral differential regulation (Oxford Instruments DTC2) of the current through a heater wound on a copper block on which the samples were mounted. Experiments were performed in the 4.2–180 K temperature range.

III. RESULTS

In Fig. 1 the erbium-related PL spectra measured for the Fz-Si:Er and Cz-Si:Er,O samples at the temperature of 4.2 K are shown. The data were obtained with laser power set to 100 mW, corresponding to power incident on the sample of about 1 mW. For the float-zone material the spectrum was taken from a sample implanted to the dose of 1×10^{13} cm⁻². This particular sample was chosen for the more detailed studies as reported here following an investigation of the PL intensity dependence on Er doses. In these preceding measurements it was observed that the intensity increases with implantation dose from 10^{12} to 10^{13} cm⁻², corresponding to erbium peak concentrations of approximately 4×10^{16} and 4×10^{17} cm⁻³, respectively, as revealed by Rutherford backscattering and secondary ion mass spectrometry.^{19,23} For higher doses the PL intensity stabilized and then decreased.

Previous studies of the erbium-related photoluminescence revealed that the spectrum measured at liquid-helium temperature consists of a high-intensity peak around the wavelength $\lambda = 1.54$ μ m, possibly having some nearly coincident components, and several lines with smaller intensity on the lower-energy side of the main feature.^{2,6–9} In oxygen-lean material usually a weaker PL spectrum with a more

complex structure than in Czochralski material is observed. From high-resolution PL studies on a wide range of erbium implanted silicon samples Jantsch *et al.*⁹ and Przybylinska *et al.*¹⁴ reported that two high-intensity lines with the wavenumbers $\sigma = 6507.5 \text{ cm}^{-1}$ ($\lambda = 1536.7 \text{ nm}$) and $\sigma = 6508.5 \text{ cm}^{-1}$ ($\lambda = 1536.5 \text{ nm}$) and the corresponding low-energy side lines, were observed in Cz-Si but not in Fz-Si. They suggested to ascribe these emissions to erbium–oxygen complexes. In Fig. 1 the four PL lines at the wavelengths $\lambda = 1538, 1556, 1575,$ and 1599 nm , respectively, marked by solid arrows, which are commonly assigned to an erbium-related center of cubic symmetry are more prominently present in Cz-Si. Other PL features, one set of eight lines marked by broken arrows, and most probably related to erbium luminescent centers of lower symmetry, appear stronger in the Fz-Si. Following the generally adopted interpretation we can conclude that in the materials as used in the present experiments spectra originating from cubic and non-cubic centers were observed. In the spectrum obtained for the Fz-Si material a noncubic center seems to prevail. For the Cz-Si:Er,O sample the emission at 1537.9 nm and side emissions of the cubic center dominate the spectrum.

The excitation power dependence of the photoluminescence intensity was measured for all four kinds of samples. Results are presented in Figs. 2(a)–2(d) for sample temperatures of 4.2 K obtained by immersing samples in liquid helium. Power dependencies are plotted in terms of normalized luminescence intensity I as a function of normalized excitation power P , as will be discussed in the next section. Results were fitted by a formula

$$I(P) = P / (1 + \beta \cdot P + P), \quad (1)$$

where β is an adjustable parameter representing the physical elements of the luminescence process. The solid lines as drawn in Fig. 2(a) for Fz-Si:Er, Fig. 2(b) for Cz-Si:Er, Fig. 2(c) for Cz-Si:Er,O, and Fig. 2(d) for a-Si:Er correspond to the computer fits by the above expression with $\beta = 2.63, 2.73, 2.25,$ and -0.25 , respectively. In these four cases a normalized power $P = 1$ corresponds to laser powers of $36, 14, 3,$ and 420 mW , respectively. For the Cz-Si doped with both erbium and oxygen the saturation level is approached most closely for lower excitation power; the amorphous silicon is most difficult to saturate. In all cases the saturation level is substantially reduced for higher temperatures, but no systematic quantitative observations were made for this effect.

Temperature dependencies of the PL intensities were measured for the three kinds of crystalline silicon samples. Figures 3(a)–3(c) show the PL intensity versus temperature as obtained for the Fz-Si:Er, Cz-Si:Er, and Cz-Si:Er,O samples, respectively. In each case the temperature dependence of the amplitude of the most intense spectral component near 1540 nm has been recorded. As can be seen, the PL intensities are rather constant in the low-temperature range and reduce gradually with increasing temperatures. Above 170 K the erbium-related luminescence was quenched to below the detection level. The experimentally established temperature dependencies of the PL intensity could be fitted with the equations

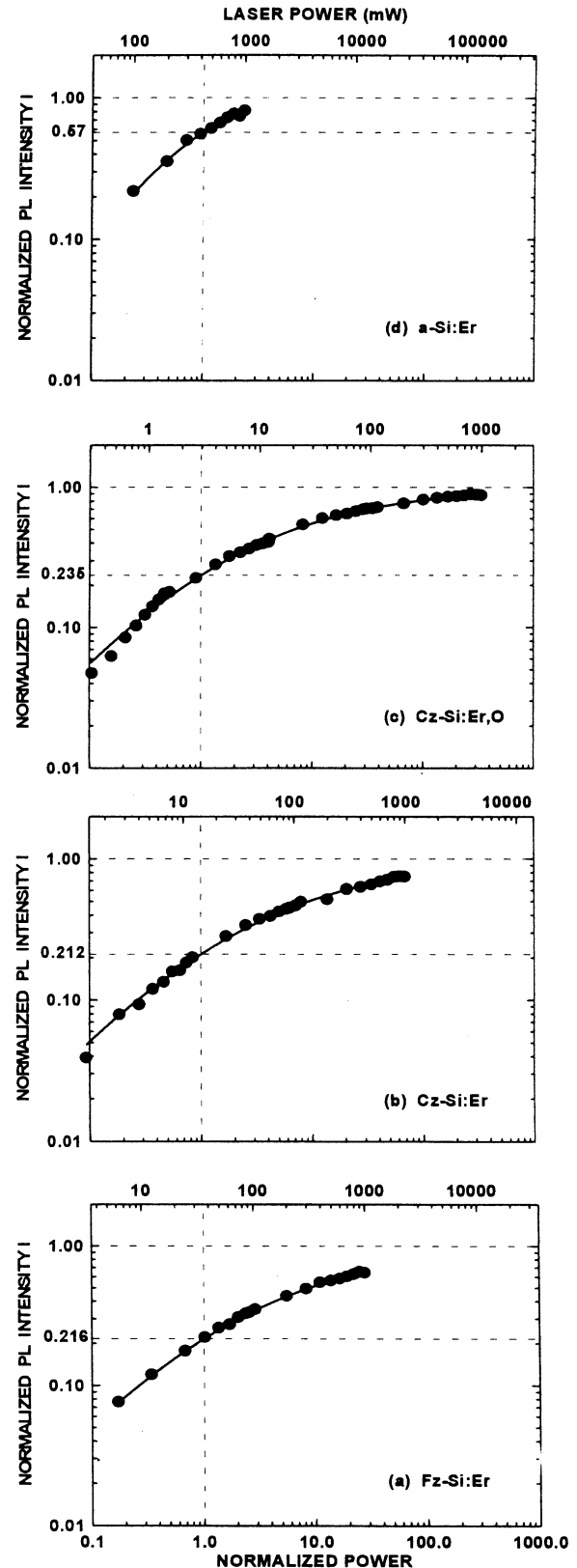


FIG. 2. Photoluminescence intensity, measured at 4.2 K , in normalized units I , as a function of excitation power for (a) Fz-Si:Er, (b) Cz-Si:Er, (c) Cz-Si:Er,O, and (d) a-Si:Er samples. Applied laser power, in units of milliwatts, is given on the top coordinate axes; normalized power P , common to all samples, is shown on the bottom axes. Experimental data points (●) and theoretical curve according to formula (1) with fitting parameter β .

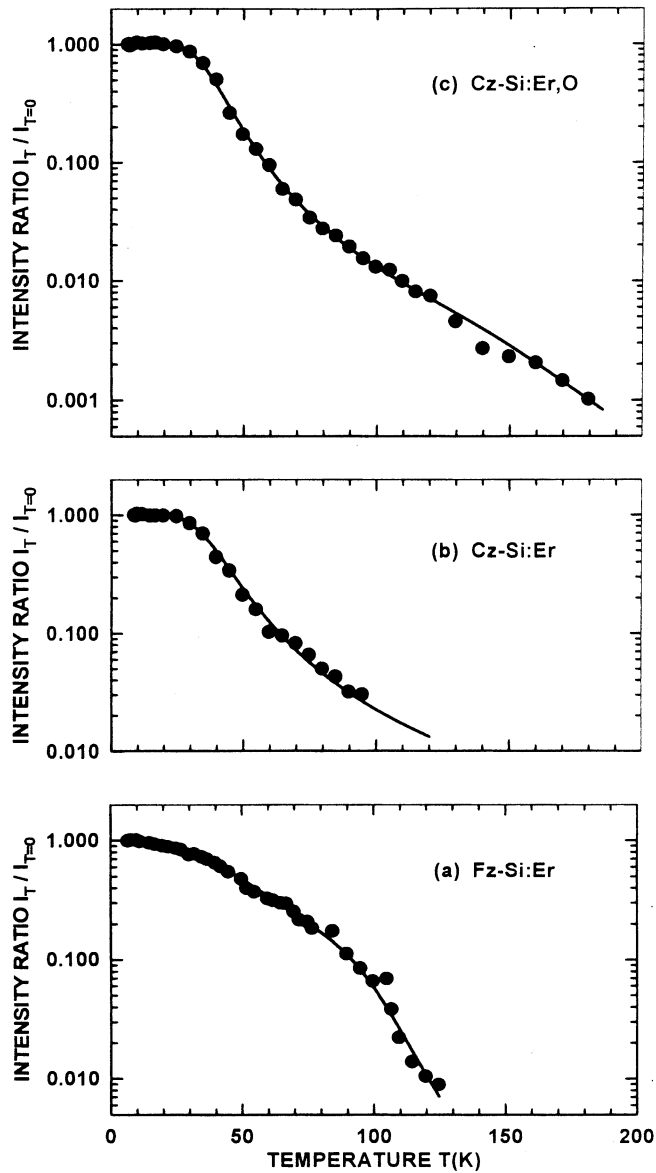


FIG. 3. Photoluminescence intensities as a function of sample temperature, normalized to the yield at low temperature, for (a) Fz-Si:Er, (b) Cz-Si:Er, and (c) Cz-Si:Er,O. The solid lines represent fits with expression (2a) using temperature-dependent pre-exponential factors.

$$I(T) = I(0) / [1 + \sum_{i=1 \dots n} A_i T^{3/2} \exp(-E_i/kT)] \quad (2a)$$

and

$$I(T) = I(0) / [1 + \sum_{i=1 \dots n} A_i \exp(-E_i/kT)], \quad (2b)$$

where the energies E_i correspond to activation energies of individual processes responsible for the temperature quenching. The particular values of the activation energies E_i and the constants A_i , as obtained from the data fitting, are summarized in Tables I and II. Data were analyzed with, but also without, as customary, a temperature factor $T^{3/2}$ included in Eqs. (2a) and (2b), anticipating the discussion in the next paragraph. The solid curves in Fig. 3 represent the computer-adjusted fits to the experimental data using expression (2a) with a $T^{3/2}$ temperature dependence explicitly included in the pre-exponential factors. As can be concluded from inspec-

TABLE I. Activation energies E_i and constants A_i derived from the temperature dependence of the photoluminescence of three different crystalline silicon samples. Fits were made using Eq. (2a) with constant A_i and temperature factor $T^{3/2}$ in the pre-exponential coefficients. Several values of laser power were used.

| Sample | Laser power (mW) | A_0 ($K^{-3/2}$) | E_0 (meV) | A_1 ($K^{-3/2}$) | E_1 (meV) | A_2 ($K^{-3/2}$) | E_2 (meV) |
|------------|------------------|----------------------|-------------|----------------------|-------------|----------------------|-------------|
| Fz-Si:Er | 100 | 0.0024 | 1.1 | 0.037 | 14.5 | 2300 | 109 |
| | 150 | | | 0.04 | 12.2 | 32 | 92 |
| | 300 | | | 0.01 | 6.6 | 3.6 | 74 |
| Cz-Si:Er | 100 | | | 0.21 | 13.6 | | |
| | 150 | | | 0.09 | 9.9 | | |
| | 200 | | | 0.07 | 10.8 | | |
| Cz-Si:Er,O | 50 | | | 0.35 | 12.9 | | |
| | 100 | | | 0.46 | 15.6 | 575 | 120 |
| | 150 | | | 0.21 | 11.4 | 1600 | 149 |

tion of results as presented in Fig. 3, two exponential terms are sufficient for a satisfactory description of the temperature dependence of the Fz and Cz samples.

IV. DISCUSSION

A. Mechanism of the photoluminescence

To understand the dependence of the erbium-related photoluminescence on temperature and excitation power the overall process of energy transfer in the erbium-doped silicon crystal must be considered. In the current, commonly accepted model this is the multistep process schematically illustrated in Fig. 4. The participating species are free electrons and holes with concentration n , free excitons with concentration n_x , erbium-bound excitons with concentration n_{xb} , and erbium ions in an excited state with concentration n_{Er}^* . The forward process of energy transfer leading to luminescence starts with the generation of free electrons and holes, to equal concentrations, at the rate G by the incident laser light. These free carriers can combine into free excitons following a second-order process with the rate $\gamma_x n^2$. Trap-

TABLE II. Activation energies E_i and constants A_i derived from the temperature dependence of the photoluminescence of three different crystalline silicon samples. Fits were made using Eq. (2b) with temperature independent constant A_i in the pre-exponential coefficients. Several values of laser power were used.

| Sample | Laser power (mW) | A_0 | E_0 (meV) | A_1 | E_1 (meV) | A_2 | E_2 (meV) |
|------------|------------------|-------|-------------|-------|-------------|-----------------|-------------|
| Fz-Si:Er | 100 | 0.7 | 3.1 | 50 | 17.6 | 2×10^6 | 107 |
| | 150 | 0.09 | 3.0 | 52 | 17.7 | 7×10^4 | 90 |
| | 300 | | | 26 | 14.4 | 4×10^5 | 122 |
| Cz-Si:Er | 100 | | | 350 | 19.8 | | |
| | 150 | | | 110 | 14.9 | | |
| | 200 | | | 100 | 15.5 | | |
| Cz-Si:Er,O | 50 | | | 1160 | 21.4 | 8×10^7 | 197 |
| | 100 | | | 950 | 22.9 | 4×10^5 | 97 |
| | 150 | | | 725 | 20.4 | 8×10^6 | 158 |

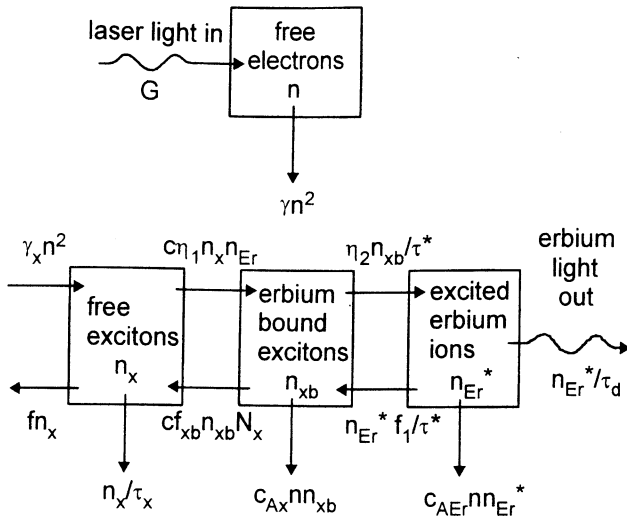


FIG. 4. Physical model for the photoexcitation of erbium luminescence showing generation and loss of free electrons n , free excitons n_x , erbium-bound excitons n_{xb} , and erbium ions in excited state n_{Er}^* . Notation $\eta_1 = (n_{Er} - n_{xb})/n_{Er}$ and $\eta_2 = (n_{Er} - n_{Er}^*)/n_{Er}$ is used.

ping of the free excitons at free erbium sites will be proportional to both exciton and the available concentration of free erbium sites. This latter concentration is written as the total erbium concentration n_{Er} multiplied by the fraction of free sites $[(n_{Er} - n_{xb})/n_{Er}]$. Erbium-bound excitons can transfer their energy in an impurity Auger process to the $4f$ electrons in the inner core of the erbium ion with a transfer time τ^* . At the same time a hot carrier accepting the excess energy E_A is formed. This process can only happen for erbium ions still in their ground state, i.e., to the fraction $[(n_{Er} - n_{Er}^*)/n_{Er}]$. At high excitation power these fractions given between the square brackets tend to zero and counteract further energy transfer. The exhaustion of the available erbium centers results in saturation of the luminescence. In the last step, the luminescence follows from decay of excited erbium ions n_{Er}^* with the time constant τ_d . The photoluminescence as measured in the experiment is proportional to this decay rate n_{Er}^*/τ_d . This decay, from an erbium $^4I_{13/2}$ excited to the $^4I_{15/2}$ ground state, is an internal atomic transition and is expected to have a temperature-independent time constant.²⁴

Reverse processes are indicated in Fig. 4 by the arrows pointing in the left direction. They include the dissociation of free excitons into free electrons and holes, the release of excitons from their erbium trapping sites and a back-transfer process in which an erbium-bound exciton is recreated starting from an excited erbium ion. In such reverse processes the energy increases and they are therefore thermally activated by energies characteristic for the distinct processes, which are in the 10–100 meV range. Reverse processes are suppressed at the lowest temperatures. They reduce the luminescence output although they do not remove energy from the luminescence path. The coefficients of forward and reverse processes, as indicated in Fig. 4, are linked by considerations of detailed balancing.

In addition to the energy transfer in the chain leading to luminescence, the full analysis of the luminescence mechanism must also include processes which act in competition,

and remove energy irreversibly from the proper path. Processes in this category are indicated in Fig. 4 by arrows pointing downwards. They include the loss of free electrons and holes via recombination centers other than the optically active erbium centers, with the rate γn^2 , e.g., due to deep levels existing as the result of implantation damage and deciding on the lifetime of the carriers. The direct recombination of free excitons or via alternative centers also leads to loss of excitation energy. In Fig. 4 two Auger processes which will remove energy from the luminescence path are also indicated. In the first one erbium-bound excitons dissipate their energy in an Auger process with the involvement of a free electron in a conduction band state. In the other process erbium ions in the excited state lose their energy by imparting it to a free electron. Both processes are thus assumed to be proportional to the free-electron concentration and proceed with rate constants c_{Ax} and c_{AEr} as indicated in Fig. 4.

It is generally assumed that erbium, and erbium-related centers, introduce donor levels in the band gap. The exact atomic and electronic nature of such centers is not known. For the erbium-related level positions at $E_{cb} - 150$ meV (Ref. 15), $E_{cb} - 170$ meV (Ref. 6), and $E_{cb} - 266$ meV (Ref. 23) have been reported. Series of levels observed at other depths, e.g., at 0.20, 0.26, 0.36, and 0.51 eV²⁵ or at 0.18, 0.23, 0.27, and 0.39 eV¹⁹ indicate that the deep-level properties depend very much on specific sample preparation conditions. Eight more levels are given by Benton *et al.*²⁶ As only the neutral erbium center is capable of binding an exciton the ionization of the donor is another way of thermal quenching of the luminescence. In the present analysis this quenching mechanism is not considered as thermal ionization of the donors is expected not to occur in the covered temperature range.

In a recent article, a model as discussed above, but not including the two Auger processes, has been put on a mathematical basis by Bresler and co-workers.¹⁷ In a steady state the concentrations are described by the balance Eq. (3) for free electrons, Eq. (4) for free excitons, Eq. (5) for bound excitons, and Eq. (6) for excited erbium ions. Following the model of Bresler *et al.* these are

$$G + fn_x = \gamma_x n^2 + \gamma n^2, \quad (3)$$

$$\gamma_x n^2 + cf_{xb} n_{xb} N_x = cn_x n_{Er} [(n_{Er} - n_{xb})/n_{Er}] + fn_x + n_x/\tau_x, \quad (4)$$

$$cn_x n_{Er} [(n_{Er} - n_{xb})/n_{Er}] + n_{Er}^* f_1/\tau^* = n_{xb} [(n_{Er} - n_{Er}^*)/n_{Er}]/\tau^* + cf_{xb} n_{xb} N_x, \quad (5)$$

and

$$n_{xb} [(n_{Er} - n_{Er}^*)/n_{Er}]/\tau^* = n_{Er}^*/\tau_d + n_{Er}^* f_1/\tau^*. \quad (6)$$

Generation terms are given in the left hand sides of these equations; loss terms appear in each case on the right hand side. Relations between the coefficients of forward and reverse processes are, as mentioned, based on detailed balancing of the separate steps. Such considerations lead to

$$f = \gamma_x (N_c N_v / N_x) \exp(-E_x/kT), \quad (7)$$

$$f_{xb} = \exp(-E_{xb}/kT)N_x \exp(-E_{xb}/kT) / [N_x \exp(-E_{xb}/kT) + n_{Er}], \quad (8)$$

and

$$f_1 = \exp(-E_A/kT). \quad (9)$$

Characteristic energies involved in these process steps appear in the equations by E_x , the binding energy of electron and hole in an exciton, E_{xb} , the energy of binding of an exciton to a neutral erbium center, and E_A , the energy dissipated in the creation of an excited erbium ion from the bound exciton situation. Densities of states in conduction, valence and exciton bands are found from the standard relations

$$N_c = 2(2\pi m_e kT/h^2)^{3/2}, \quad (10)$$

$$N_v = 2(2\pi m_h kT/h^2)^{3/2}, \quad (11)$$

and

$$N_x = 2(2\pi m_x kT/h^2)^{3/2}, \quad (12)$$

with the relevant effective masses. An exact solution of the balance equations, in the form of a quadratic equation for n_{Er}^*/n_{Er} , was given by Bresler *et al.*

B. Excitation power dependence

1. Energy transfer without Auger processes

Measurements of the power dependence of the luminescence intensity, as reported in this article, were performed at liquid-helium temperature. At this low temperature the reverse processes, all requiring thermal activation, are suppressed, which expressed in the mathematical form means $f = f_{xb} = f_1 = 0$. For the balance equations valid at low temperature one obtains

$$G = \gamma_x n^2 + \gamma n^2, \quad (3a)$$

$$\gamma_x n^2 = c n_x n_{Er} [(n_{Er} - n_{xb})/n_{Er}] + n_x / \tau_x, \quad (4a)$$

$$c n_x n_{Er} [(n_{Er} - n_{xb})/n_{Er}] = n_{xb} [(n_{Er} - n_{Er}^*)/n_{Er}] / \tau^*, \quad (5a)$$

and

$$n_{xb} [(n_{Er} - n_{Er}^*)/n_{Er}] / \tau^* = n_{Er}^* / \tau_d. \quad (6a)$$

The concentration of excited erbium ions n_{Er}^* is found as the solution of

$$a_0 (n_{Er}^*/n_{Er})^2 - (b_0 + b_2 G) (n_{Er}^*/n_{Er}) + c_2 G = 0 \quad (13)$$

with the coefficients

$$a_0 = 1 + c n_{Er} \tau_x [1 + (\tau^*/\tau_d)], \quad (13a)$$

$$b_0 = 1 + c n_{Er} \tau_x, \quad (13b)$$

$$b_2 = \gamma_x \tau_x c \tau_d [1 + (\tau^*/\tau_d)] / (\gamma_x + \gamma), \quad (13c)$$

and

$$c_2 = \gamma_x \tau_x c \tau_d / (\gamma_x + \gamma). \quad (13d)$$

In its general form, the equation predicts saturation of n_{Er}^*/n_{Er} for high excitation power G at the level $n_{Er}^*/n_{Er} = c_2/b_2$. For low power a linear relationship $n_{Er}^*/n_{Er} = (c_2/b_0)G$ is expected. When comparing predictions of the model equations with experimental data one must be aware

that neither the generation power nor the luminescence output are easily known in absolute numbers to good accuracy. For instance, the doping of the sample may be spatially non-uniform and the volume in which excitation takes place is not well defined. The fraction of optically active erbium centers may be much less than one, which is still a matter of investigation. Such uncertain factors are likely to change from sample to sample. For such reasons it is of advantage to eliminate these factors by resorting to relative units. As regards the luminescence intensity the most natural unit at hand for normalization is the saturation value c_2/b_2 . A normalized intensity is therefore introduced as $I \equiv (n_{Er}^*/n_{Er})/(c_2/b_2)$. For the excitation power a unit G_1 is obtained as the value at which the extrapolated linear increase at low power crosses the saturation level. This will be for $G_1 = b_0/b_2$. Also the normalized power $P \equiv G/G_1$ is a dimensionless quantity. In terms of the normalized units Eq. (13) acquires the simple form

$$I^2 - \alpha(1+P)I + \alpha P = 0, \quad (14)$$

with

$$\alpha \equiv b_0 b_2 / a_0 c_2. \quad (14a)$$

It thus appears that the dependence of the intensity I on the generation power P is governed by the one parameter α , through which all aspects of the luminescence process are represented. However, from Eq. (14) it is easily concluded that for low power $I = P$, and for high power $I = 1$, irrespective the value of parameter α . This implies that, when considered in normalized form, the parameters a_0 , b_0 , b_2 , and c_2 , or the more basic physical coefficients γ , γ_x , c , f , f_{xb} , f_1 , τ_x , τ^* , and τ_d , have no effect on the power dependence in the low- and high-power regions. Only at intermediate power, i.e., at $P \approx 1$, the results will depend on α . Only in the transition region between linear increase and saturation the observed luminescence does reveal insight into the luminescence process. The most typical value to study the luminescence mechanism is therefore at power $P = 1$. At this excitation level the luminescence intensity is given by

$$I = \alpha - (\alpha^2 - \alpha)^{1/2}. \quad (15)$$

From the equality $\alpha = b_0 b_2 / a_0 c_2$ and the parameters as given by Eqs. (13a)–(13d) one concludes that $1 \leq \alpha \leq \infty$. For such values of α always solutions from Eq. (15) do exist. For $\alpha = 1$ one obtains $I_{P=1} = 1$ and for $\alpha = \infty$ one has $I_{P=1} = 0.5$. The range of possible luminescence intensities at unit power $P = 1$ consistent with Eq. (14) is restricted between 0.5 and 1. For these limiting values the intensity versus power curves for an extended range are drawn in Fig. 5(a).

In Fig. 5(a) experimental data are also included. They result from the measurements at liquid-helium temperature on four samples with the different specifications as given in Sec. II. In all cases the luminescence intensity was followed as a function of excitation power over the maximum accessible range. Experimental data are plotted for normalized power $P = 1$ at the observed values $I = 0.216$ for Fz-Si:Er, $I = 0.212$ for Cz-Si:Er, and $I = 0.235$ for Cz-Si:Er,O. Obviously, these are all outside the range of results as can be described by the model. For the *a*-Si material, on the other

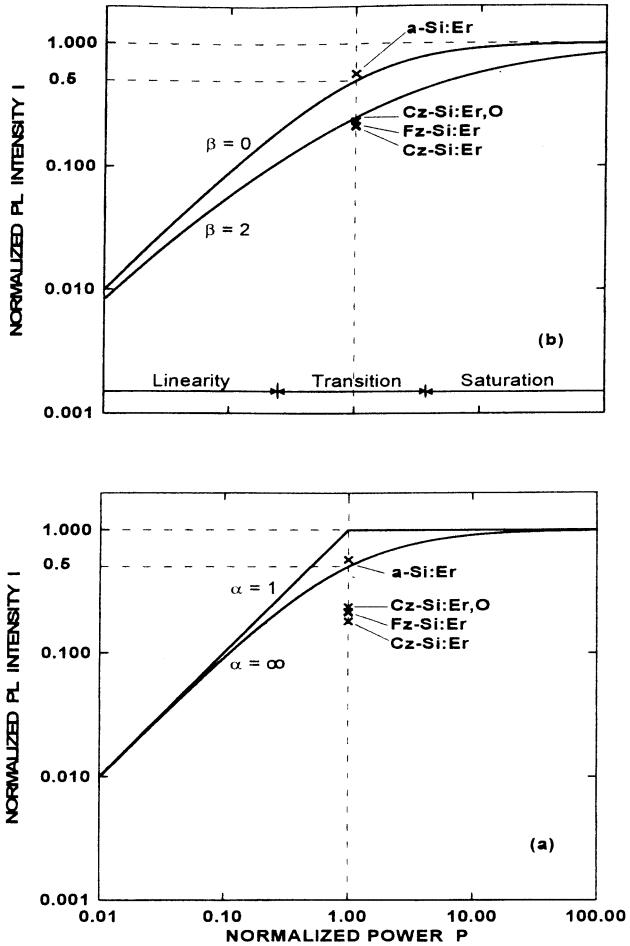


FIG. 5. Normalized luminescence output I as a function of normalized laser input P , (a) as predicted by model equations without Auger processes for lowest and highest values of parameter α . (b) for the model including strong Auger decay processes for process parameter $\beta=0$ and $\beta=2$. The transition region in which the term $\beta \cdot P$ dominates in the denominator of Eq. (20) is indicated for $\beta=2$. Experimental data points (X) for the four samples are given for unit power $P=1$.

hand, the observed $I=0.57$, corresponding to $\alpha=2.32$, represents an available solution. Further interpretation of this result, using Eqs. (14a) and (13a)–(13d) leads to the requirement that both conditions $\tau^*/\tau_d > 1.32$ and $1/cn_{Er}\tau_x > 1.32$ must hold. As this is not likely to be the case, the validity of the model also for the a -Si is doubtful.

2. Energy transfer with Auger processes

One has to conclude that the presented model is not able to provide the quantitative description of the luminescence process. In order to improve the model energy losses through Auger processes involving conduction band electrons may be considered, as has been suggested before by Palm *et al.*¹⁸ The two processes are indicated in Fig. 4. In the balance Eqs. (5a) and (6a) they are implemented by including on the loss side the Auger rates $c_{Ax}nn_{xb}$ and $c_{AEr}nn_{Er}^*$. The extended balance equations for the bound excitons and the erbium ions in excited state become, respectively,

$$cn_x n_{Er} [(n_{Er} - n_{xb})/n_{Er}] = n_{xb} [(n_{Er} - n_{Er}^*)/n_{Er}] / \tau^* + c_{Ax} nn_{xb}, \quad (5b)$$

and

$$n_{xb} [(n_{Er} - n_{Er}^*)/n_{Er}] / \tau^* = n_{Er}^* / \tau_d + c_{AEr} nn_{Er}^*. \quad (6b)$$

In order to solve the new set of equations [Eqs. (3a), (4a), (5b), and (6b)] it is helpful to introduce appropriate simplifications. Considering numerical values one may assume that the loss of free electrons and holes is dominated by their recombination via traps with rate γn^2 . The loss via exciton formation $\gamma_x n^2$ is comparatively much less. Under such conditions the energy transfer model can be broken up into two parts. In stream I the balance of electrons is considered separately by Eq. (3a). The loss of electrons through exciton formation is ignored in this mainstream. At low temperature this leads to

$$G = (\gamma_x + \gamma)n^2, \quad (16)$$

and

$$n = [G / (\gamma_x + \gamma)]^{1/2}. \quad (17)$$

The electron concentration obtained via this solution is used to describe the Auger processes. Typical numbers are $G = 10^{22} \text{ cm}^{-3} \text{ s}^{-1}$, $\gamma_x = 10^{-12} \text{ cm}^3 \text{ s}^{-1}$, $\gamma = 10^{-10} \text{ cm}^3 \text{ s}^{-1}$, and $n = 10^{16} \text{ cm}^{-3}$, corresponding to an electron lifetime of $1 \mu\text{s}$.

In energy stream II the balance of free excitons, bound excitons, and excited erbium ions is separately considered. Solution of the equations leads to a cubic equation in n_{Er}^*/n_{Er} , which, accepting some approximation,²⁷ can be factorized to yield a quadratic equation

$$(a_0 + a_1 G^{1/2} + a_2 G)(n_{Er}^*/n_{Er})^2 - (b_0 + b_1 G^{1/2} + b_2 G + b_3 G^{3/2})(n_{Er}^*/n_{Er}) + c_2 G = 0, \quad (18)$$

with

$$a_0 = 1 + cn_{Er}\tau_x [1 + (\tau^*/\tau_d)], \quad (18a)$$

$$a_1 = c_{AEr}\tau_d [1 + cn_{Er}\tau_x + 2cn_{Er}\tau_x(\tau^*/\tau_d)] / (\gamma_x + \gamma)^{1/2}, \quad (18b)$$

$$a_2 = cn_{Er}\tau_x(\tau^*/\tau_d)(c_{AEr}\tau_d)^2 / (\gamma_x + \gamma), \quad (18c)$$

$$b_0 = 1 + cn_{Er}\tau_x, \quad (18d)$$

$$b_1 = (1 + cn_{Er}\tau_x)(c_{AEr}\tau_d + c_{Ax}\tau^*) / (\gamma_x + \gamma)^{1/2}, \quad (18e)$$

$$b_2 = \{ (1 + cn_{Er}\tau_x)c_{AEr}\tau_d c_{Ax}\tau^* + \gamma_x \tau_x c \tau_d [1 + (\tau^*/\tau_d)] \} / (\gamma_x + \gamma), \quad (18f)$$

$$b_3 = \gamma_x \tau_x c \tau_d c_{AEr}\tau_d (\tau^*/\tau_d) / (\gamma_x + \gamma)^{3/2}, \quad (18g)$$

and

$$c_2 = \gamma_x \tau_x c \tau_d / (\gamma_x + \gamma). \quad (18h)$$

At low power the model equations reflect the linear increase $n_{Er}^*/n_{Er} = (c_2/b_0)G$, just as before. At high power, however, the consistent solution $n_{Er}^*/n_{Er} = (c_2/b_3)/G^{1/2}$ predicts decreasing luminescence intensity upon increase of the excitation level G . Such a behavior is to be expected, as in the adopted model two independent saturation mechanisms are active. In the first one the concentration of erbium-bound excitons, n_{xb} , is driven towards the concentration of available erbium ions but cannot exceed this concentration. The second saturation mechanism is the combined action of the

two Auger processes. At high power, and hence high concentrations of free electrons, the Auger mechanism removing excited erbium ions nonradiatively becomes very effective. This will result in a reduction of n_{Er}^* , which becomes proportional to $1/n$, or $1/G^{1/2}$. Such a decrease has not been observed in the present experiments; it has also not been reported in the literature. Inspection of the equations shows that one should expect the decrease to set in at excitation values where $c_{\text{AEr}}\tau_d(\tau^*/\tau_d)(G/\gamma)^{1/2} > 1$. Considering numerical values ($c_{\text{AEr}} \approx 10^{-12} \text{ cm}^3 \text{ s}^{-1}$, $\tau^* \approx 4 \times 10^{-6} \text{ s}$) this corresponds to high values of G , near and above $10^{26} \text{ cm}^{-3} \text{ s}^{-1}$, which are not reached in actual experiments. This can be attributed to the small value of (τ^*/τ_d) , as τ^* is in the range of microseconds and τ_d is of order milliseconds. Introducing the approximation $\tau^*/\tau_d \approx 0$, Eqs. (18) reduce in many respects to Eqs. (13). In particular the term $b_3 G^{3/2}$ in Eq. (18) is lost and the equation predicts saturation at c_2/b_2 . Both for low and for high power an approximate solution of Eq. (18) will be

$$n_{\text{Er}}^*/n_{\text{Er}} = c_2 G / (b_0 + b_1 G^{1/2} + b_2 G). \quad (19)$$

This result will also be valid for intermediate power if the Auger processes are strong ($c_{\text{AEr}}n\tau_d > 1$, $c_{\text{Ax}}n\tau^* > 1$). Following solution (19) for this special case one has saturation at c_2/b_2 , linear increase at low power with $(c_2/b_0)G$, and $G_1 = b_0/b_2$. Expressing Eq. (19) in terms of normalized units, as before, the result will read

$$I = P / (1 + \beta P^{1/2} + P) \quad (20)$$

with

$$\beta \equiv b_1 / (b_0 b_2)^{1/2}, \quad (20a)$$

or

$$\beta = (c_{\text{AEr}}\tau_d + c_{\text{Ax}}\tau^*) / [c_{\text{AEr}}\tau_d c_{\text{Ax}}\tau^* + \gamma_x \tau_x c \tau_d / (1 + c n_{\text{Er}} \tau_x)]^{1/2}. \quad (20b)$$

Under the assumed condition of strong Auger effect this reduces to

$$\beta = (c_{\text{AEr}}\tau_d + c_{\text{Ax}}\tau^*) / (c_{\text{AEr}}\tau_d c_{\text{Ax}}\tau^*)^{1/2}, \quad (20c)$$

or

$$\beta = (c_{\text{AEr}}\tau_d / c_{\text{Ax}}\tau^*)^{1/2} + (c_{\text{Ax}}\tau^* / c_{\text{AEr}}\tau_d)^{1/2}. \quad (20d)$$

As usual, the power dependence of the luminescence has its linear increase at low power with $I = P$ and saturates at high power at $I = 1$. Features of the luminescence process are only revealed at intermediate power, e.g., at $P = 1$, where $I = 1/(2 + \beta)$. For a general case parameter β will be positive following Eq. (20b); for the case of strong Auger effect $\beta \geq 2$, as follows from Eqs. (20c) or (20d). Figure 5(b) illustrates the curves as obtained from Eq. (20) for $\beta = 0$ and $\beta = 2$. Curves for $\alpha = \infty$ in Fig. 5(a) and $\beta = 0$ in Fig. 5(b) are identical, both representing $I = P/(1 + P)$. Compared to the previous case, without Auger effect, the transition region between linear behavior and saturation is broader. This is due to the appearance of the $P^{1/2}$ term which in this model is a fingerprint of the Auger effect.

Considering again the experiment, the measured data for the luminescence power dependence of samples of the four

types are plotted in Fig. 2. The solid curves are best fits to the experimental data using Eq. (20) with parameter $\beta = 2.63$ for Fz-Si:Er, $\beta = 2.73$ for Cz-Si:Er, $\beta = 2.25$ for Cz-Si:Er,O, and $\beta = -0.25$ for a-Si:Er. The data points for the four samples for $P = 1$ are also plotted in Fig. 5(b). The results for the three crystalline samples are quite similar with $\beta = 2.5 \pm 0.25$. With Eq. (20d) the result is converted to $(c_{\text{AEr}}\tau_d / c_{\text{Ax}}\tau^*)^{\pm 1} \approx 4 \pm 1$. This compares favorably with data as published in the literature, e.g., $c_{\text{AEr}} = 10^{-12} \text{ cm}^3 \text{ s}^{-1}$, $\tau_d = 10^{-3} \text{ s}$, $c_{\text{Ax}} = 10^{-10} \text{ cm}^3 \text{ s}^{-1}$, and $\tau^* = 4 \times 10^{-6} \text{ s}$.¹⁸ From the present analysis one can only conclude that $c_{\text{AEr}}\tau_d / c_{\text{Ax}}\tau^*$ is very similar for the three kinds of crystalline material investigated. This can be due to an accidental combination of parameters, but one is tempted to believe that all four parameters of erbium-related process steps, i.e., c_{AEr} , τ_d , c_{Ax} , and τ^* , have similar values. Such a conclusion, very speculative at this stage, is, however, supported in quite a good quantitative manner by available experimental data and theoretical modeling of the erbium-related luminescence process. This will be discussed, in terms of the parameters τ_d , τ^* , c_{AEr} , and c_{Ax} in the next four paragraphs.

Erbium-related luminescence follows from the radiative $^4I_{13/2}$ to $^4I_{15/2}$ transition with the emission of a photon of around 800 meV energy. Such an electric-dipole transition is parity forbidden in the spherical potential of a free atom. For an erbium ion embedded in a silicon crystal the transition will become allowed due to the lower symmetry of the crystal-field potential, which will be tetrahedral or lower depending on the specific structure of the luminescent center. As a matter of fact, one should therefore expect the decay time constant to depend on the defect structure. Crystal-field induced effects are directly manifested in the multiple-line structure of the optical spectrum. It turns out that crystal-field induced splittings are similar in magnitude for all observed optical centers. They are always in the range of 200–300 cm^{-1} . For the centers in the samples of the present experiment this is shown in Fig. 1. Results of measurements of decay time τ_d following pulsed excitation of the Fz-Si:Er and Cz-Si:Er samples of this experiment are illustrated by Fig. 6. In these experiments conditions were chosen to ensure that the spontaneous radiative lifetime τ_d is measured. Measurements were carried out with samples at low temperature and in the dark during luminescence decay. With the consequent absence of free carriers the Auger decay $c_{\text{AEr}}n\tau_d$ is effectively suppressed. At the low temperature, with $f_1 = 0$, also the back-transfer process is not effective. Auger recombinations with electrons or holes bound to shallow donors or acceptors also cannot take place to any significant extent as the doping level is below 10^{16} cm^{-3} .²⁸ From our measurements lifetimes between 500 and 2000 μs are derived. The result matches well with data known from the literature. Hartung *et al.* report lifetimes of 870 and 1060 μs , respectively, for different optically active centers in their research,²⁴ similar to a value of 1020 μs given by Taguchi *et al.*²⁹ A somewhat larger time constant $\tau_d = 1300 \mu\text{s}$ is given by Palm *et al.*¹⁸ Priolo *et al.* find lifetimes in the range 800–2000 μs , adding the comment that the lifetime of 2000 μs might be the largest lifetime ever observed for spontaneous radiative decay.²⁸ In most cases the decay deviates from

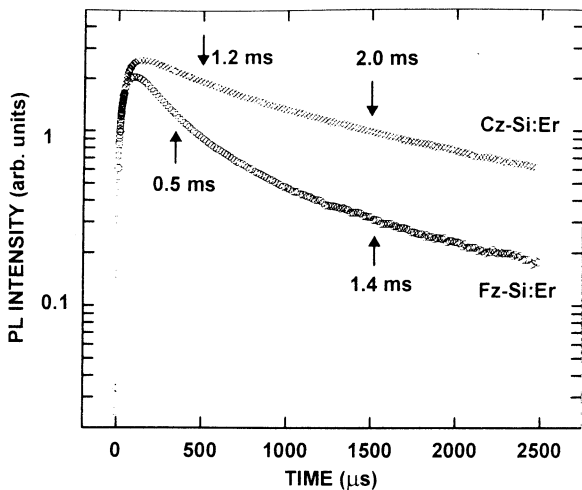


FIG. 6. Decay of the Si:Er photoluminescence at 1.54 μm of the samples Fz-Si:Er and Cz-Si:Er, measured at 5 K in the dark, following pulsed excitation at time $t = 0$. Effective decay time constants are given near the curves after short and long decay. Observed rise times reflect time constants of the detection system.

the purely exponential form when considered over a period of time of several milliseconds and is better described by two time constants, both in the above-given range. This illustrates that lifetimes can, to a minor extent, be defect specific. Such a behavior was also found for the present Cz-Si:Er and Fz-Si:Er samples, as indicated in Fig. 6; it is in agreement with the more complex structure of the luminescence spectra as shown in Fig. 1.

The time constant τ^* for energy transfer from the erbium-bound exciton to the $4f$ electrons of erbium is expected to be much shorter. For this time constant surprisingly large values were nevertheless reported, such as 30 μs by Shin *et al.*,³⁰ 50 μs by Gregorkiewicz *et al.*,³¹ and 100 μs by Przybylinska *et al.*³² Very recently it was argued by Taguchi *et al.*²⁹ that such values reflect the time constants of the detection system rather than those of erbium-related processes. The true value of τ^* is substantially smaller but has not been measured in a large number of cases yet due to the instrumental requirement of having a detection system which at the same time is both very sensitive and fast. Values close to 1 μs given in the literature by Bresler *et al.*,¹⁷ Taguchi *et al.*,²⁹ and Palm *et al.*¹⁸ represent the most reliable estimates of τ^* . In the present analysis the value of Palm *et al.*, $\tau^* = 4 \mu\text{s}$, has been selected as it is based on experimental determination.

The treatment of the Auger recombination coefficient can be put on a solid theoretical basis. In a pioneering work by Suchocki and Langer³³ the relation

$$c_{\text{AEr}} = 1/n_0 \tau_d \quad (21)$$

with

$$n_0 = 4 \pi^{5/2} n_r^5 [(m_0/m_e) a_0 / \alpha]^{1/2} \lambda^{-7/2} \quad (22)$$

was derived for the impurity Auger effect with free carriers. Inserting in this expression $n_r = \epsilon_r = 3.4$ for silicon, $m_e = 0.3m_0$ the effective mass of a conduction band electron, $a_0 = 5.29 \text{ nm}$ the Bohr radius, $\alpha = 1/137.036$ the Sommerfeld

fine-structure constant, and $\lambda = 1.54 \mu\text{m}$ the wavelength of the radiation, the value $n_0 = 1.2 \times 10^{15} \text{ cm}^{-3}$ is obtained. With the radiative lifetime put equal to 1 ms, the Auger coefficient becomes $c_{\text{AEr}} = 8 \times 10^{-13} \text{ cm}^3 \text{ s}^{-1}$. This yields an excellent agreement with experimentally determined values of $10^{-12} \text{ cm}^3 \text{ s}^{-1}$ by Palm *et al.*¹⁸ and $5 \times 10^{-13} \text{ cm}^3 \text{ s}^{-1}$ from Priolo *et al.*²⁸ It is important to note that this result only depends on the specific nature of the erbium center through the wavelength of emission λ , which is known to be a constant $\lambda = 1.54 \mu\text{m}$ in all cases.

A similar derivation can be given for the decay of erbium-bound excitons by an Auger process. A major difference is that in this electron-hole-electron recombination process the effect of electron-hole correlation enhances the probability of the Auger process considerably, as discussed by Hangleiter and Häcker.³⁴ From a numerical analysis an enhancement factor near 100 was determined in an empirical approach.¹⁸ With this procedure one obtains $c_{\text{Ax}} = 10^{-10} \text{ cm}^3 \text{ s}^{-1}$. Also in this case it can be emphasized that the result depends only on fundamental physics constants and silicon material parameters, with no dependence on the specific nature of the erbium defect.

The striking conclusion of remarkable similarity of the erbium-related emission, due to centers with different microscopic structure, thus gains confidence by an evaluation of the relevant physical parameters. The probable difference in structure of the luminescent centers in the three materials has rather limited influence on the later steps in the photoluminescence process as depicted in Fig. 4. In particular, any special role of oxygen in the formation of suitable luminescent centers is not borne out by the results. The conclusion of very similar luminescence properties of the crystalline samples, as reported here, is entirely a result of the introduction of the normalized units. Considered in terms of direct experimental units for excitation and yield, as is common practice, the results would have looked rather different. A conclusion of different behavior of the luminescent centers in these three materials is then easily, but erroneously, made. The result for the *a*-Si sample is different. To fit the experimentally observed power dependence with expression (20), parameter β has to be given the negative value $\beta = -0.25$, incompatible with Eq. (20b). One can conclude that the assumption of strong Auger effect leading to the solution (19) is not valid in the case of the amorphous silicon.

Returning to absolute units, the laser excitation power corresponding to the unit of normalized power, $P = 1$, is different for the four samples. The values, which can be taken from the top coordinate axes in Figs. 2(a)–2(d), are 36 mW for Fz-Si:Er, 14 mW for Cz-Si:Er, 3 mW for Cz-Si:Er,O, and 422 mW for the *a*-Si samples. In terms of the model equations unit power G_1 is given by

$$G_1 = b_0/b_2, \quad (23)$$

which can be approximated by

$$G_1 \approx \gamma/c_{\text{AEr}} \tau_d c_{\text{Ax}} \tau^*. \quad (24)$$

In view of this result, the different values for the unit of excitation power can easily be related to specific sample conditions, even for equal values of the parameters c_{AEr} , τ_d ,

c_{Ax} , and τ^* . The parameter γ is influenced by the presence of recombination centers in and near the excited volume, and therefore related to implantation damage and annealing treatments. Impurities, such as oxygen, either from the crystal growth or from implantation, will have their effects. Considering this factor, one may expect that in the *a*-Si the free-electron and -hole lifetime is shorter due to a higher recombination rate γ . A lower steady state electron concentration will make the luminescence excitation less probable and more excitation energy will be required to reach the saturation region. Lower electron concentration will also reduce the reaction rate of the Auger processes, in agreement with the earlier conclusion. As such parameters are not under precise control, the results, which are not vastly different for the crystalline samples, will not be subjected to further quantitative analysis.

For an order-of-magnitude evaluation of Eq. (24) the conditions of the experiment have to be considered in more detail. In the experimental setup a power set to 10 mW on the laser unit, the typical unit power for the crystalline samples, resulted in about 100 μ W of light power incident on the sample. Given the wavelength 514 nm of the Ar⁺ laser light, with associated photon energy of 2.4 eV, and assuming a 100% quantum efficiency, this light energy will yield an electron-hole generation rate of around $2.5 \times 10^{14} \text{ s}^{-1}$. Assuming a penetration depth of 1 μ m of the light in the sample and a spot size of 1 mm², the volume in which the excitation takes place is very roughly estimated at 10^{-6} cm^3 . The generation parameter G_1 for a 10 mW excitation will then be $G_1 = 2.5 \times 10^{20} \text{ cm}^{-3} \text{ s}^{-1}$. An evaluation of the right hand side of Eq. (24) will give, with $\gamma = 10^{-10} \text{ cm}^3 \text{ s}^{-1}$ and parameters c_{Aer} , τ_d , c_{Ax} , and τ^* as before, precisely this number. Under these generation-recombination conditions the electron and hole concentrations will be $n = 1.6 \times 10^{15} \text{ cm}^{-3}$ and their lifetime 6 μ s. Corresponding values for the *a*-Si sample are $G_1 = 10^{22} \text{ cm}^{-3} \text{ s}^{-1}$, $\gamma = 4 \times 10^{-8} \text{ cm}^3 \text{ s}^{-1}$, $n = 1.6 \times 10^{15} \text{ cm}^{-3}$ and the shorter lifetime 0.15 μ s confirming expectations.

C. Temperature dependence

For an analysis of the temperature dependence of the luminescence intensity one has to return to Eqs. (3)–(12). Following the conclusion of the previous section the Auger processes through which erbium-bound excitons and erbium ions in the excited state decay must be incorporated in the description. This is implemented by adding to the balance Eqs. (5) and (6) the Auger loss rates $c_{Ax}nn_{xb}$ and $c_{Aer}nn_{Er}^*$, respectively, resulting in

$$\begin{aligned} c n_x n_{Er} [(n_{Er} - n_{xb})/n_{Er}] + n_{Er}^* f_1 / \tau^* \\ = n_{xb} [(n_{Er} - n_{Er}^*)/n_{Er}] / \tau^* + c f_{xb} n_{xb} N_x + c_{Ax} n n_{xb} \end{aligned} \quad (5c)$$

and

$$\begin{aligned} n_{xb} [(n_{Er} - n_{Er}^*)/n_{Er}] / \tau^* = n_{Er}^* / \tau_d + n_{Er}^* f_1 / \tau^* \\ + c_{Aer} n n_{Er}^* . \end{aligned} \quad (6c)$$

A practical solution of these equations is again facilitated by accepting the two-stream model in which the chain of lumi-

nescence processes is considered to be a small perturbation only of the electron-hole generation by the laser light. In this model the electron concentration is given by Eq. (17). The concentrations of free and bound excitons and of excited erbium ions are found from the solution of Eqs. (4), (5c), and (6c). As before, a cubic equation for n_{Er}^*/n_{Er} is obtained, which, accepting some approximations,²⁷ can be factorized, leading to the quadratic Eq. (18), however, with the generalized temperature-dependent coefficients

$$a_0 = 1 + c n_{Er} \tau_x [1 + (\tau^*/\tau_d) + f_1] + f \tau_x, \quad (25a)$$

$$\begin{aligned} a_1 = c_{Aer} \tau_d [1 + c n_{Er} \tau_x + 2 c n_{Er} \tau_x (\tau^*/\tau_d) + f \tau_x \\ + c n_{Er} \tau_x f_1] / (\gamma_x + \gamma)^{1/2}, \end{aligned} \quad (25b)$$

$$a_2 = c n_{Er} \tau_x (\tau^*/\tau_d) (c_{Aer} \tau_d)^2 / (\gamma_x + \gamma), \quad (25c)$$

$$\begin{aligned} b_0 = 1 + c n_{Er} \tau_x + f \tau_x + c N_x \tau_d f_{xb} (1 + f \tau_x) \\ \times [(\tau^*/\tau_d) + f_1], \end{aligned} \quad (25d)$$

$$\begin{aligned} b_1 = [(1 + c n_{Er} \tau_x + f \tau_x) (c_{Aer} \tau_d + c_{Ax} \tau^* + f_1 c_{Ax} \tau_d) \\ + (1 + f \tau_x) c_{Aer} \tau_d c N_x \tau^* f_{xb}] / (\gamma_x + \gamma)^{1/2}, \end{aligned} \quad (25e)$$

$$\begin{aligned} b_2 = \{ \gamma_x \tau_x c \tau_d [1 + (\tau^*/\tau_d) + f_1] \\ + c_{Aer} \tau_d c_{Ax} \tau^* (1 + c n_{Er} \tau_x + f \tau_x) \} / (\gamma_x + \gamma), \end{aligned} \quad (25f)$$

$$b_3 = \gamma_x \tau_x c \tau_d c_{Aer} \tau_d (\tau^*/\tau_d) / (\gamma_x + \gamma)^{3/2}, \quad (25g)$$

and

$$c_2 = \gamma_x \tau_x c \tau_d / (\gamma_x + \gamma). \quad (25h)$$

Assuming avoidance of exceeding saturation and the presence of strong Auger effect, as discussed before, the solution given in Eq. (19) will again be applicable. At low temperature Eqs. (25a)–(25h) will reduce to those of Eqs. (18a)–(18h) and give the solution $(n_{Er}^*/n_{Er})_{T=0}$. For the practical purpose of comparing model predictions with results of experiments it is useful to express measured intensities at arbitrary temperature in the intensity as observed at low temperature, i.e., in the normalized unit $(n_{Er}^*/n_{Er})_T / (n_{Er}^*/n_{Er})_{T=0}$, or $(n_{Er}^*)_T / (n_{Er}^*)_{T=0}$. As a solution one finally obtains

$$\begin{aligned} (n_{Er}^*)_T / (n_{Er}^*)_{T=0} \\ = 1 / \{ 1 + A_x \exp[-E_x/kT] + A_{xb} \exp[-E_{xb}/kT] \\ + A_{xbx} \exp[-(E_{xb} + E_x)/kT] + A_A \exp[-E_A/kT] \\ + A_{Ax} \exp[-(E_A + E_x)/kT] + A_{Axb} \exp[-(E_A + E_{xb})/ \\ kT] + A_{Axbx} \exp[-(E_A + E_{xb} + E_x)/kT] \}. \end{aligned} \quad (26)$$

The result is of the form as anticipated by Eqs. (2a) and (2b) and comprises all possible combinations of the activation energies E_x , E_{xb} , and E_A . For brevity the lengthy expressions for the coefficients A will not be given here.²⁷ With the general expression (26) experimental data can be analyzed, but in view of the large number of adjustable parameters no unique determination of them can be expected. To be more specific the magnitude of the various terms in the denominator should be critically considered. It appears that all terms which include the activation energy E_x are proportional to $f \tau_x$. Using Eq. (7), an evaluation shows that the $f \tau_x$ product

is expected to be small compared to unity in the temperature range below 100 K. As a consequence the four corresponding terms in Eq. (26) can be dropped. In terms of physics this approximation implies that the decay of free excitons by direct recombination, proportional to $1/\tau_x$, is much faster than the process of their dissociation with the rate f , in the considered temperature range. The steady state exciton concentration is dictated by direct decay, not by the thermal equilibrium with free electrons and holes. In the experiment the thermal dissociation of excitons does not play a role. Hence, its activation energy disappears from the equations and is not measured. Of the remaining terms in Eq. (26) an estimate of values shows that $A_A < A_{Axb}$, allowing the neglect of the term $A_A \exp[-E_A/kT]$. This latter approximation is, however, of small practical relevance for the analysis of data. For the actual analysis of temperature dependence the curtailed form of Eq. (26) is used

$$(n_{Er^*})_T / (n_{Er^*})_{T=0} = 1 / \{ 1 + A_{xb} \exp[-E_{xb}/kT] + A_{Axb} \exp[-(E_A + E_{xb})/kT] \}. \quad (27)$$

The coefficients are

$$A_{xb} = cN_x \tau_x^* / (1 + cn_{Er} \tau_x) (1 + \rho^{1/2} P^{1/2}) \quad (27a)$$

and

$$A_{Axb} = cN_x \tau_d / (1 + cn_{Er} \tau_x) (1 + \beta P^{1/2} + P) \quad (27b)$$

with the introduction of parameter $\rho \equiv c_{Ax} \tau_x^* / c_{AEr} \tau_d$. The parameters β and ρ also appeared in the analysis of excitation power dependence; their numerical values were determined in the previous paragraph and were found not to deviate far from one. The results as following from Eq. (27) show that the temperature dependence is a function of excitation power. Under conditions of saturation the thermal quenching will be absent. At low power the relation

$$A_{xb} = (\tau_x^* / \tau_d) A_{Axb} \quad (28)$$

is established by the model.

Analysis of the data on temperature dependence as obtained in this investigation is based on Eq. (27). Rewriting this equation in the form

$$(n_{Er^*})_{T=0} / (n_{Er^*})_T - 1 = A_{xb} \exp[-E_{xb}/kT] + A_{Axb} \exp[-(E_A + E_{xb})/kT] \quad (29)$$

shows that the curves as given in Fig. 7 are predicted to be the sum of two exponential functions. From the results as shown in Fig. 7 for the three kinds of samples it is concluded that in the temperature range below typically 100 K one exponential process contributes. This process, with an activation energy around 10–20 meV is identified with the term $A_{xb} \exp[-E_{xb}/kT]$ of Eq. (29). At temperatures above 100 K the data points deviate from the straight line in the positive sense as a manifestation of the term $A_{Axb} \exp[-(E_A + E_{xb})/kT]$ which has the higher activation energy and becomes effective only at high temperature. In this region the luminescence intensity has already decreased to low levels

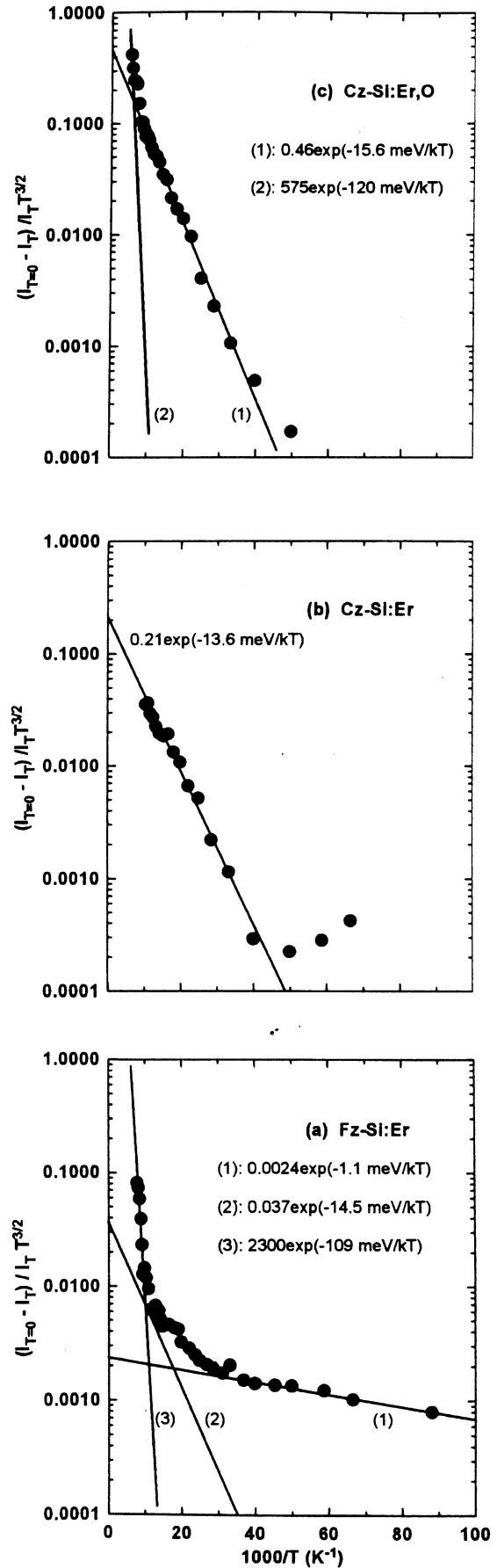


FIG. 7. Plots of $(I_{T=0} - I_T) / I_T T^{3/2}$ as a function of reciprocal temperature illustrating the analysis based on Eq. (29) for (a) Fz-Si:Er, (b) Cz-Si:Er, and (c) Cz-Si:Er,O.

and is measured with less accuracy. As also fewer data points are available in the narrow temperature range 100–170 K the parameters A_{Axb} and $E_A + E_{xb}$ cannot be determined with high accuracy. For the energies an error limit of at least 10 meV has to be accepted. Actual data taken for the three crystalline samples at a few excitation power levels in the intermediate power region were analyzed in this manner. The analyses could be successfully carried out with two exponential contributions. Only in the case of sample Fz-Si:Er a third term with a small activation energy around 1 meV was helpful to improve the fit. The origin of this term is not clear. In the case of sample Cz-Si:Er the higher-temperature region where the term $A_{Axb} \exp[-(E_A + E_{xb})/kT]$ starts to contribute was not reached. Given the satisfactory quality of the fits achieved over the whole temperature range, as also illustrated by Fig. 3, an extension of Eq. (29) so as to include more exponential processes appears to be meaningless. Numerical results for the parameters are given in Tables I and II. Due to the appearance of N_x , the density of states in the exciton band, in Eqs. (27a) and (27b) both A_{xb} and A_{Axb} include a $T^{3/2}$ temperature dependence. For this reason, such an analysis has been given preference. In the literature, however, analyses with temperature-independent pre-exponential coefficients prevail. The alternative analysis has therefore also been made, with results given in Table II. Although inconsistent with the model prescription, the quality of such fits was not worse at all. On comparing the activation energies in the two tables, differences of several millielectron volts, sometimes amounting to near 50%, are observed. This hampers the spectroscopic identification of the processes involved. Values for E_{xb} are found to be different for the three samples, suggestive for exciton binding to erbium-related centers with a different structure. Only one energy in the range 10–20 meV is required for analyses. The absence of the E_x activation energy connected with exciton dissociation is confirmed by this result. Following the analysis, the larger activation energy is identified with $E_A + E_{xb}$ leading to the experimental result $E_A \approx 80$ meV. By the physical model E_A is given as $E_A = E_g - E_x - E_{xb} - E_{PL} - E_d$. In order to satisfy the experimental result, and with estimates for the silicon band gap energy $E_g = 1170$ meV, electron-hole binding energy in a free exciton $E_x = 15$ meV, exciton binding energy to erbium center $E_{xb} = 15$ meV, luminescence energy $E_{PL} = 800$ meV, a donor ionization energy is required of $E_d = 260$ meV. This is close to the level position at 266 meV as reported in Ref. 23 for the same Fz-silicon as used in the present experiments. As usual, the determination of pre-exponential factors has larger uncertainties. From Eqs. (27a) and (27b) order-of-magnitude estimates $A_{xb}/T^{3/2} \approx 1$ and $A_{Axb}T^{3/2} \approx 10^3$ can be made, in rough agreement with the parameters as given in Table I. The experimental results also tend to support the prediction that for higher excitation powers the temperature dependence is weaker.

V. CONCLUSION

The dependence of the photoluminescence intensity of erbium-doped silicon in the 1.54 μm spectrum on excitation power and temperature has been experimentally measured

and analyzed. For the analysis a model was used in which the incident light energy is transferred via the intermediate stages of free electrons and holes, free excitons, and erbium-bound excitons to the intra-4*f*-shell excited erbium ions. In order to explain the power dependence, it was found to be necessary to include Auger processes by which erbium-bound excitons and excited erbium ions decay into the model. A remarkable similarity was found for crystalline samples of float-zone and Czochralski origin. In these materials the probable structural difference in the luminescent centers appears to have no strong effect on the relevant properties of erbium-bound excitons, erbium ions in the excited states, their interactions, or their decay, radiatively or by Auger processes. Differences in sample behavior are mainly associated with the earlier stages of the energy transfer process related to electrons, holes and excitons, and their trapping and recombination. This conclusion was revealed by the consistent use of normalized units for both excitation power and luminescent intensity. The thermal dependence is governed by the binding energy of excitons to erbium centers in the temperature range below 100 K. The energy of binding electrons and holes together in an exciton does not have an effect on the temperature dependence and is hence not measured. At higher temperatures, above around 100 K, an activation energy near 100 meV becomes more prominent. This energy is associated with the transfer of energy from an excited erbium ion back to an erbium-bound exciton. Typical medium electron-hole excitation rates in the experiments are estimated at $10^{22} \text{ cm}^{-3} \text{ s}^{-1}$. A consistent analysis of experimental results for power and temperature dependence was carried out with parameter values $\gamma_x = 10^{-12} \text{ cm}^3 \text{ s}^{-1}$, $\gamma = 10^{-10} \text{ cm}^3 \text{ s}^{-1}$, $c = 5 \times 10^{-10} \text{ cm}^3 \text{ s}^{-1}$, $c_{Ax} = 10^{-10} \text{ cm}^3 \text{ s}^{-1}$, $c_{AEr} = 10^{-12} \text{ cm}^3 \text{ s}^{-1}$, $\tau_x = 5 \times 10^{-6} \text{ s}$, $\tau^* = 4 \times 10^{-6} \text{ s}$, and $\tau_d = 10^{-3} \text{ s}$.

ACKNOWLEDGMENTS

Samples for the reported experiments were kindly provided by F. P. Widdershoven, Philips Research, Eindhoven, The Netherlands, by N. A. Sobolev and I. N. Yassievich, A. F. Ioffe Physico-Technical Institute, St. Petersburg, Russia, and L. C. Kimerling and J. Michel, MIT, Cambridge, MA.

¹In *Rare Earth Doped Semiconductors*, edited by G. S. Pomrenke, P. B. Klein, and D. W. Langer (Materials Research Society, Pittsburgh, PA, 1993); in *Rare Earth Doped Semiconductors II*, edited by S. Coffa, A. Polman, and R. N. Schwarz (Materials Research Society, Pittsburgh, PA, 1996).

²Y. S. Tang, K. C. Heasman, W. P. Gillin, and B. J. Sealy, *Appl. Phys. Lett.* **55**, 432 (1989).

³Y. S. Tang, Z. Jingping, K. C. Heasman, and B. J. Sealy, *Solid State Commun.* **72**, 991 (1989).

⁴U. Wahl, A. Vantomme, J. De Wachter, R. Moons, G. Langouche, J. G. Marques, J. G. Correia, and ISOLDE Collaboration, *Phys. Rev. Lett.* **79**, 2069 (1997).

⁵V. F. Masterov and L. F. Zakharenkov, *Sov. Phys. Semicond.* **24**, 383 (1990) [translation from *Fiz. Tekh. Poluprovodn.* (St. Petersburg) **24**, 610 (1990)].

⁶J. Michel, J. L. Benton, R. F. Ferrante, D. C. Jacobson, D. J. Eaglesham, E. A. Fitzgerald, Y.-H. Xie, J. M. Poate, and L. C. Kimerling, *J. Appl. Phys.* **70**, 2672 (1991).

⁷J. Michel, L. C. Kimerling, J. L. Benton, D. J. Eaglesham, E. A. Fitzgerald, D. C. Jacobson, J. M. Poate, Y.-H. Xie, and R. F. Ferrante, *Mater. Sci. Forum* **83–87**, 653 (1992).

- ⁸I. de Maat-Gersdorf, T. Gregorkiewicz, C. A. J. Ammerlaan, and N. A. Sobolev, *Semicond. Sci. Technol.* **10**, 666 (1995).
- ⁹W. Jantsch, G. Hendorfer, M. Bruckner, L. Palmethofer, and H. Przybylinska, in *The Physics of Semiconductors*, edited by D. J. Lockwood (World Scientific, Singapore, 1995), p. 2411.
- ¹⁰P. N. Favennec, H. L'Haridon, D. Moutonnet, M. Salvi, and M. Gauneau, *Jpn. J. Appl. Phys., Part 2* **29**, L524 (1990).
- ¹¹P. N. Favennec, H. L'Haridon, D. Moutonnet, M. Salvi, and M. Gauneau, in *Rare Earth Doped Semiconductors*, edited by G. S. Pomrenke, P. B. Klein, and D. W. Langer (Materials Research Society, Pittsburgh, PA, 1993) p. 181.
- ¹²D. L. Adler, D. C. Jacobson, D. J. Eaglesham, M. A. Marcus, J. L. Benton, J. M. Poate, and P. H. Citrin, *Appl. Phys. Lett.* **61**, 2181 (1992).
- ¹³H. Przybylinska, G. Hendorfer, M. Bruckner, L. Palmethofer, and W. Jantsch, *Appl. Phys. Lett.* **66**, 490 (1995).
- ¹⁴H. Przybylinska, W. Jantsch, Yu. Suprun-Belevitch, M. Stepikhova, L. Palmethofer, G. Hendorfer, A. Kozanecki, R. J. Wilson, and B. J. Sealy, *Phys. Rev. B* **54**, 2532 (1996).
- ¹⁵F. Priolo, G. Franzò, S. Coffa, A. Polman, S. Libertino, R. Barklie, and D. Carey, *J. Appl. Phys.* **78**, 3874 (1995).
- ¹⁶H. Efeoglu *et al.*, *Semicond. Sci. Technol.* **8**, 236 (1993).
- ¹⁷M. S. Bresler, O. B. Gusev, B. P. Zakharchenya, and I. N. Yassievich, *Phys. Solid State* **38**, 813 (1996) [translation from *Fiz. Tverd. Tela (Leningrad)* **38**, 1474 (1996)].
- ¹⁸J. Palm, F. Gan, B. Zheng, J. Michel, and L. C. Kimerling, *Phys. Rev. B* **54**, 17 603 (1996).
- ¹⁹F. P. Widdershoven, Phd. thesis, University Twente, The Netherlands (1991).
- ²⁰N. A. Sobolev, *Semiconductors* **29**, 595 (1995) [translation from *Fiz. Tekh. Poluprovodn. (St. Petersburg)* **29**, 1153 (1995)].
- ²¹N. A. Sobolev, O. V. Alexandrov, V. V. Emtsev, M. I. Makoviichuk, A. V. Merkulov, E. O. Parshin, D. S. Poloskin, and E. I. Shek, *Solid State Phenom.* **47-48**, 299 (1996).
- ²²M. S. Bresler, O. B. Gusev, V. Kh. Kudoyarova, A. N. Kuznetsov, P. E. Pak, E. I. Terukov, I. N. Yassievich, B. P. Zakharchenya, W. Fuhs, and A. Sturm, *Appl. Phys. Lett.* **67**, 3599 (1995).
- ²³F. P. Widdershoven and J. P. M. Naus, *Mater. Sci. Eng. B* **4**, 71 (1989).
- ²⁴J. Hartung, J. H. Evans, P. Dawson, A. P. Scholes, T. Taskin, M. Q. Huda, C. Jeynes, and A. R. Peaker, in *Rare Earth Doped Semiconductors II*, edited by S. Coffa, A. Polman, and R. N. Schwarz (Materials Research Society, Pittsburgh, PA, 1996), p. 119.
- ²⁵S. Libertino, S. Coffa, G. Franzò, and F. Priolo, *J. Appl. Phys.* **78**, 3867 (1995).
- ²⁶J. L. Benton, J. Michel, L. C. Kimerling, D. C. Jacobson, Y.-H. Xie, D. J. Eaglesham, E. A. Fitzgerald, and J. M. Poate, *J. Appl. Phys.* **70**, 2667 (1991).
- ²⁷D. T. X. Thao, Phd. thesis, University of Amsterdam, The Netherlands (2000).
- ²⁸F. Priolo, G. Franzò, S. Coffa, and A. Camera, *Phys. Rev. B* **57**, 4443 (1998).
- ²⁹A. Taguchi, K. Takahei, M. Matsuoka, and S. Tohno, *J. Appl. Phys.* **84**, 4471 (1998).
- ³⁰J. H. Shin, G. N. van den Hoven, and A. Polman, *Appl. Phys. Lett.* **67**, 377 (1995).
- ³¹T. Gregorkiewicz, I. Tsimperidis, C. A. J. Ammerlaan, F. P. Widdershoven, and N. A. Sobolev, in *Rare Earth Doped Semiconductors II*, edited by S. Coffa, A. Polman, and R. N. Schwarz (Materials Research Society, Pittsburgh, PA, 1996), p. 207.
- ³²H. Przybylinska, G. Hendorfer, M. Bruckner, W. Jantsch, and L. Palmethofer, *J. Alloys Compd.* **225**, 555 (1995).
- ³³A. Suchocki and J. M. Langer, *Phys. Rev. B* **39**, 7905 (1989).
- ³⁴A. Hangleiter and R. Häcker, *Phys. Rev. Lett.* **65**, 215 (1990).